JCB Article

MuSK is required for anchoring acetylcholinesterase at the neuromuscular junction

Annie Cartaud,[1] Laure Strochlic,[1] Manuel Guerra,[2] Benoît Blanchard,[1] Monique Lambergeon,[2] Eric Krejci,[2] Jean Cartaud,[1] and Claire Legay[2]

[1]Biologie Cellulaire des Membranes, Institut Jacques Monod, UMR 7592 Centre National de la Recherche Scientifique (CNRS), Universités Paris 6 and Paris 7, 75251 Paris, Cedex 05, France
[2]Neurobiologie Moléculaire et Cellulaire, Ecole Normale Supérieure, UMR 8544 CNRS, 75230 Paris, Cedex 05, France

At the neuromuscular junction, acetylcholinesterase (AChE) is mainly present as asymmetric forms in which tetramers of catalytic subunits are associated to a specific collagen, collagen Q (ColQ). The accumulation of the enzyme in the synaptic basal lamina strictly relies on ColQ. This has been shown to be mediated by interaction between ColQ and perlecan, which itself binds dystroglycan. Here, using transfected mutants of ColQ in a ColQ-deficient muscle cell line or COS-7 cells, we report that ColQ clusterizes through a more complex mechanism. This process requires two heparin-binding sites contained in the collagen domain as well as the COOH terminus of ColQ. Cross-linking and immunoprecipitation experiments in *Torpedo* postsynaptic membranes together with transfection experiments with muscle-specific kinase (MuSK) constructs in MuSK-deficient myotubes or COS-7 cells provide the first evidence that ColQ binds MuSK. Together, our data suggest that a ternary complex containing ColQ, perlecan, and MuSK is required for AChE clustering and support the notion that MuSK dictates AChE synaptic localization at the neuromuscular junction.

Introduction

Acetylcholinesterase (AChE; EC 3.1.1.7) terminates neurotransmission by hydrolyzing acetylcholine at cholinergic synapses. The accumulation of AChE in the synaptic cleft is a prerequisite for a tight control in time and space of the cholinergic neurotransmission.

At the vertebrate neuromuscular junction (NMJ), much of the AChE is a collagen-tailed enzyme also called asymmetric form (A form; Legay, 2000). This molecular form corresponds to tetramers of $AChE_T$ subunits associated to a specific collagen called collagen Q (ColQ; Krejci et al., 1991, 1997). ColQ is a collagen in which the central collagenous domain is flanked by specific NH_2 and COOH terminus peptides. Trimers of ColQ associate in a triple helix tail. With increasing levels of $AChE_T$, tetramers of catalytic subunits fill one, two, or three strands of this collagen tail and are referred as A_4, A_8, and A_{12} according to the number of catalytic subunits per collagen tail. At the NMJ, most of the enzyme is present as A_{12} forms. The association between tetramers of AChE and ColQ relies on the interaction between the tryptophan amphiphilic tetramerization domain contained in the COOH terminus of the $AChE_T$ subunit and a proline-rich domain (PRAD) contained in the NH_2 terminus of ColQ (Bon et al., 1997; Simon et al., 1998).

Several lines of evidences have progressively focused on ColQ as being responsible for the accumulation of the enzyme at the NMJ. Indeed, the enzyme has been shown to be tightly bound to the synaptic basal lamina and most of the enzyme can be removed by treatment of the muscle with collagenase (Hall and Kelly, 1971; McMahan et al., 1978). More recently, the analysis of ColQ-deficient mutant mice generated by a disruption of the sequence encoding the PRAD in the ColQ gene has shown that no clusters of AChE can be detected at the NMJ (Feng et al., 1999). Congenital myasthenic syndromes associated with AChE deficiency all result from recessive mutations in ColQ (Engel et al., 2003). Therefore, the AChE accumulation in the synaptic cleft relies entirely on ColQ.

Address correspondence to Claire Legay, Laboratoire de neurobiologie Mol, 46 rue d'Ulm, 75230 Paris, Cedex 05, France. Tel.: 33-1-42-86-20-68. email: claire.legay@univ-paris5.fr

Key words: synapse; cholinergic transmission; perlecan; ColQ; heparin-binding sites

Abbreviations used in this paper: AChE, acetylcholinesterase; AChR, acetylcholine receptor; A form, asymmetric form; ColQ, collagen Q; HBS, heparin-binding sites; HSPG, heparan sulfate proteoglycan; MALDI-TOF, matrix-assisted laser desorption ionization-time of flight; MT, myotube; MuSK, muscle-specific kinase; NMJ, neuromuscular junction; PRAD, proline-rich domain; wt, wild-type.

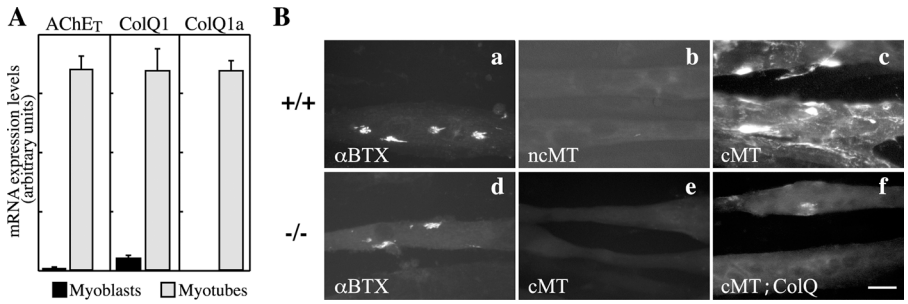

Figure 1. **Expression of AChE and ColQ in mouse wt and ColQ-deficient myogenic cells in culture.** (A) AChE$_T$, ColQ1, and ColQ1a mRNAs levels were quantified by real-time RT-PCR (±SEM) in wt myoblasts and MTs. AChE$_T$ mRNAs levels were increased by 130-fold average and ColQ1 mRNAs levels by 20-fold average after differentiation into MTs. ColQ1a transcripts were only detectable in MTs. Note that the bars do not allow direct comparison between the different transcripts. (B) Cultures were stained with either α-bungarotoxin (a and d, αBTX) or the A63 polyclonal rat anti-AChE antibody (b, c, e, and f). Wt and ColQ-deficient MTs formed AChR clusters (a and d). AChE clusters did not form in noncontracting MTs (b, ncMT) and were only revealed in contracting MTs (c, cMT). No AChE clusters were detected in ColQ-deficient contracting MTs (e). Transfection of ColQ-deficient MTs with rat ColQ1a restores the ability of these cells to form AChE clusters in contracting MTs (f). Bar, 20 μm.

During formation of the vertebrate NMJ, several mechanisms contribute to the postsynaptic differentiation. They include preferential expression of a class of genes by synaptic nuclei, lateral diffusion-trap of receptors in the membrane, or increased stability of synaptic proteins within clusters. The heparan sulfate proteoglycan (HSPG) agrin released by the nerve terminal orchestrates the maintenance of most of these processes. The role of agrin has mainly been dissected through the accumulation of acetylcholine receptors (AChRs). In brief, agrin activates a tyrosine kinase receptor called muscle-specific kinase (MuSK), which is specifically concentrated at the postsynaptic membrane. The activation of MuSK induces a cascade of signal transduction events through rapsyn leading to the formation of AChR clusters (Sanes and Lichtman, 2001; Burden, 2002).

Local expression of AChE mRNAs has also been shown to be responsible for the high expression level of the enzyme at the NMJ in all types of muscles (Jasmin et al., 1993; Legay et al., 1995). The pattern of ColQ mRNAs expression is more complex. Two variants of ColQ called ColQ1 and ColQ1a that both contain the PRAD are synthesized by the muscle fibers (Krejci et al., 1999). Both ColQ1a and ColQ1 mRNAs are present all along the muscle fiber in slow muscles whereas ColQ1a mRNAs are highly accumulated around the synaptic nuclei in fast muscles. The association of AChE with ColQ has been shown to generate metabolic stabilization of the enzyme (Legay et al., 1999). Given the high concentration of AChE mRNAs at the synapse, it explains that most of the collagen present at the synapse is saturated with tetramers of AChE (A_{12} forms). Once secreted, A forms interact with HSPGs in the ECM. Indeed, the enzyme is partly solubilized by heparin and binding of purified exogenous A_{12} on sections of NMJ is blocked by heparin (Brandan et al., 1985; Rotundo et al., 1997). The interaction between ColQ and HSPGs is only mediated by two clusters of basic residues located in the collagen domain (Deprez and Inestrosa, 1995; Deprez et al., 2003). Perlecan, a major HSPG at the NMJ, colocalizes with AChE in clusters and binds only to A forms of AChE suggesting that it participates in ColQ clustering (Peng et al., 1999). This role of perlecan is further supported by the analysis of perlecan-null mice in which AChE is undetectable in the NMJ (Arikawa-Hirasawa et al., 2002). In turn, perlecan binds dystroglycan, a transmembrane protein of the sarcolemma concentrated at the NMJ (Jacobson et al., 2001). Therefore, AChE is anchored in the synaptic basal lamina through the scaffold ColQ–perlecan-dystroglycan. It remains that heparin or high salt containing buffers only extract newly formed collagen-tailed AChE (Rossi and Rotundo, 1996). These results suggested that an other component but HSPG is stabilizing the hetero-oligomer in the synaptic basal lamina. Several mutations in the ColQ COOH terminus domain have been shown to hinder the accumulation of AChE at the synapse and lead to a myasthenic syndrome associated with AChE deficiency (Donger et al., 1998; Ohno et al., 1998, 2000). These mutations do not impede the formation of the triple helix of collagen nor the association of ColQ with AChE. Furthermore, the deletion of the ColQ COOH terminus domain does not affect the relative affinity of this mutant protein for heparin and this domain does not interact with heparin (Deprez et al., 2003). These observations prompted us to hypothesize that beside the interaction with perlecan, other molecular interactions through the COOH terminus domain of ColQ may be involved in the accumulation of AChE. Here, we have analyzed the respective roles of each of the two heparin-binding sites (HBS) which are known to have different biochemical properties and the COOH terminus domain in ColQ clustering. We also have searched for the molecular partner interacting with ColQ COOH terminus. First, we demonstrate that both the HBS and the COOH terminus domain of ColQ are involved in the accumulation of the enzyme in clusters. Second, we show that ColQ binds MuSK through its COOH terminus.

Results

Expression of AChE and ColQ in muscle cells

We first asked whether the expression of AChE and the two variants of ColQ, ColQ1, and ColQ1a is regulated during muscle differentiation. For this purpose, we used time-lapse RT-PCR to quantify the levels of the specific mRNAs in myoblasts and myotubes (MTs) in culture. To test whether the absence of ColQ influences AChE gene expression during differentiation, the quantification was done on RNAs extracted from a wild-type (wt) and from a ColQ-deficient myogenic cell line that we have generated. Data show that AChE and ColQ1 mRNAs were up-regulated after fusion of myoblasts by 130- and 20-fold, respectively, in wt muscle cells (Fig. 1 A). Thus, the induction of ColQ1 variant upon

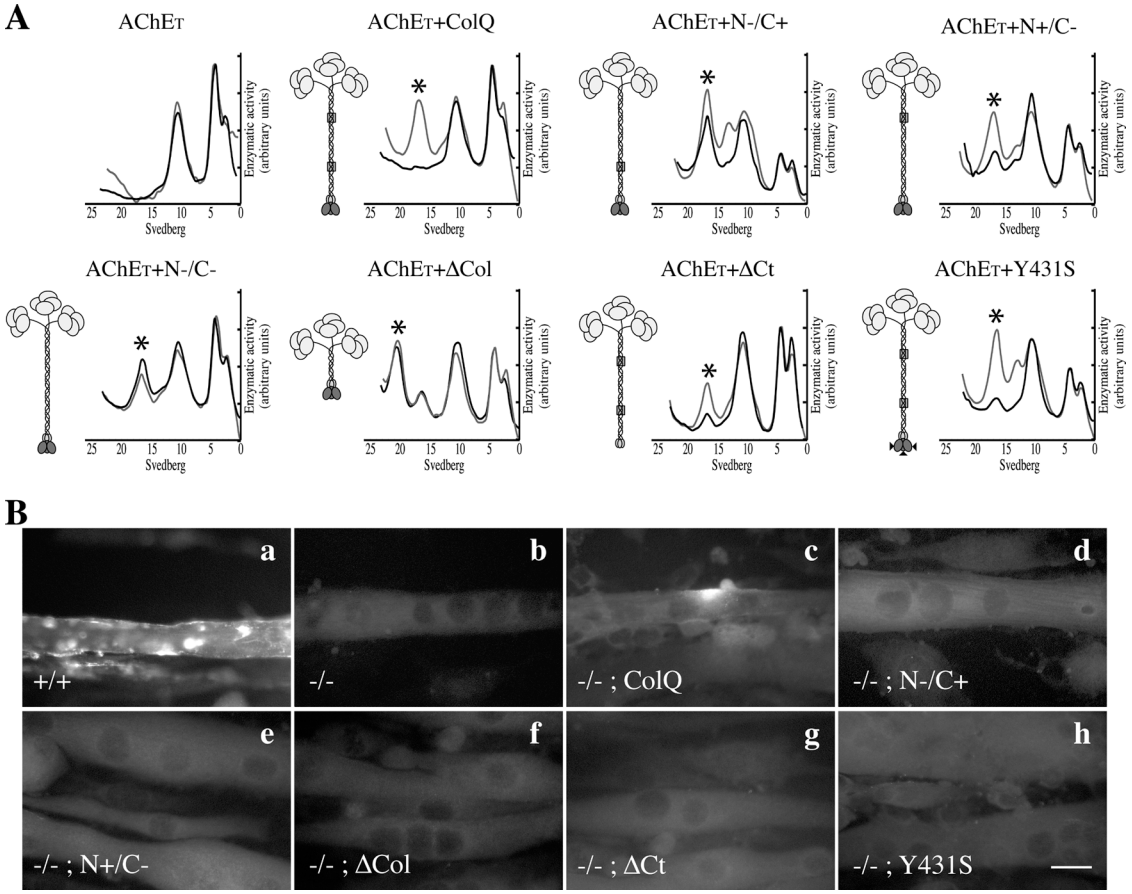

Figure 2. **Distinct sites of ColQ are necessary for the formation of AChE clusters.** (A) Analysis of AChE molecular forms secreted from the ColQ-deficient myogenic cells transfected with $AChE_T$ or cotransfected with $AChE_T$ and wt ColQ or ColQ mutants. Sedimentation profiles of the molecular forms are shown in black lines. Asterisk indicates the position of A_{12} forms in the sedimentation profiles. Co-transfected cells were also treated for 24 h by heparin. Sedimentation profiles of the molecular forms secreted after heparin treatment are shown in gray lines. A schematic representation of AChE A forms and ColQ mutant constructs used in this work are shown on the left side of the gradients. Catalytic subunits (ovoids) are associated to a triple helix of ColQ. This last protein contains a collagen domain (186–285 aa) flanked by a NH_2-terminal peptide (1–186 aa) and a COOH-terminal peptide (285–450 aa). The two HBS (N^+ and C^+) contained in the collagen domain are indicated as gray boxes. In mutant construct N^-/C^+, RK (121–122 aa) is mutated to DP. In mutant construct N^+/C^-, KR (226–227 aa) is mutated to DP. In construct N^-/C^-, both sites are mutated. In mutant ΔCol, amino acids 105–276 were deleted. In mutant ΔCt, amino acids 362–450 were deleted. The rat Y431S construct reproduces the missense mutation detected in the human ColQ COOH terminus domain. As shown, none of the mutations prevented the formation and secretion of AChE A forms. (B) Cells were labeled with antibodies to AChE. Wt myogenic cells (+/+) formed AChE clusters (a), whereas no AChE clusters were detected in myogenic cells derived from ColQ-deficient mice (−/−; b). ColQ transfected in ColQ-deficient muscle cells restored the formation of AChE clusters (c), but no AChE clusters were detected when these cells were transfected with either the N^-/C^+ construct (d), the N^+/C^- construct (e), the ΔCol construct (f), the ΔCt construct (g), or the Y431S construct (h).

differentiation was much lower than the one observed for AChE in these muscle cells. The ColQ1a variant was expressed in wt MTs but could not be detected in wt myoblasts (Fig. 1 A). In ColQ-deficient muscle cells, AChE mRNAs were increased by 180-fold in a range nonsignificantly different from that observed in wt myogenic cells (unpublished data). This result suggests that the absence of ColQ in ColQ-deficient cells does not modify the expression level of AChE mRNAs. None of the two ColQ variants were detected in ColQ-deficient muscle cells (unpublished data).

Expression of exogenous ColQ in ColQ-deficient cell lines restores clusters of AChE

Soon after fusion of the MTs, spontaneous AChR clusters were detected on wt and $ColQ^{-/-}$ MTs (Fig. 1 B, a and d). However, AChE aggregates did not form in wt MTs until muscle cell contraction occurred a week average after fusion (Fig. 1 B, b and c). This result can be correlated with a dramatic increase in AChE and ColQ mRNAs expression (unpublished data) detected concomitantly with muscle cell contraction or a process of late differentiation. AChE aggregates were not present at the surface of $ColQ^{-/-}$ MTs even when these MTs were contracting (Fig. 1 B, e). Because the ColQ1a variant seems to be mostly expressed at the synapse and is only present in differentiated muscle cells, we transfected ColQ-deficient myoblasts at confluence with ColQ1a and induced fusion of the myoblasts the next day. AChE aggregates were observed in approximately half of the contracting muscle cells (Fig. 1 B, f). This result indicates (a) that the presence of ColQ is an absolute prerequisite for the formation of AChE

spontaneous aggregates; (b) that ColQ is able to associate with endogenous AChE; and (c) that ColQ can restore the ability of ColQ deficient cells to produce AChE clusters. Finally, AChR aggregates form independently from those of AChE.

The two HBS and the COOH terminus of ColQ are necessary for the formation of ColQ clusters

To determine the relative functions of the two HBS and the COOH terminus domain of ColQ in the formation of ColQ clusters, we transfected ColQ deficient muscle cells with a series of constructs in which one of the two HBS located in N− (N−/C+) or COOH terminus (N+/C−) or both HBS (N−/C−) within the collagen domain or the main region of the collagen domain (ΔCol) or the 88 aa of the COOH terminus domain of ColQ (ΔCt) were mutated or deleted. All these mutants are described in a previous article (Deprez et al., 2003). We also generated a rat mutated ColQ cDNA (Y431S) that reproduced the human point mutation Y431S in the COOH terminus domain described previously (Donger et al., 1998). The six mutants used in this work are schematically represented in Fig. 2 A. To ascertain that these ColQ mutants were expressed and secreted by ColQ-deficient myogenic cells, we cotransfected these cells with wt or mutant ColQ and AChE. We then analyzed the AChE molecular forms secreted in the medium by the sucrose gradient technique. Because Rossi and Rotundo (1996) showed that heparin solubilizes newly synthetized A forms, we also analyzed the AChE molecular forms in the medium after treatment of the cells with heparin. As shown on Fig. 2 A, all these mutants were expressed and were able to associate with AChE to form hetero-oligomers that were secreted in the medium. Note that the ΔCol mutant presented higher sedimentation coefficients consistent with a decrease asymmetry of the molecules due to a shortened collagen tail.

As shown on Fig. 2 B, wt MTs formed AChE clusters (a) whereas no AChE clusters could be detected in ColQ deficient MTs (b). Transient transfections of MTs with wt ColQ1a restored AChE clusters (c) but neither the N−/C+ mutant (d), the N+/C− mutant (e), the N−/C− mutant (unpublished data), the ΔCol mutant (f), the ΔCt mutant (g), nor the Y431S mutant (h) was able to restore AChE clusters. Thus, because all the mutants can be targeted to the cell surface, we can conclude that spontaneous AChE clustering requires the presence of each of the two HBS as well as the COOH terminus of ColQ. AChE clusters were still detected 2–3 wk after ColQ transfection. This could be linked to the presence of high level of ColQ 10 d after transfection (not depicted) and the stability of the A forms in the ECM. Alternatively, ColQ expression in some MTs days after transfection could result from spontaneous integration events of ColQ cDNA in the genome.

The collagenic tail of AChE is linked to MuSK in *Torpedo* postsynaptic membrane

To identify MuSK partners in *Torpedo* electrocyte in situ, we have performed chemical cross-linking experiments in postsynaptic membrane purified from *Torpedo* electric tissue (Strochlic et al., 2001). Several cross-linked products containing MuSK were identified using antibodies to MuSK by

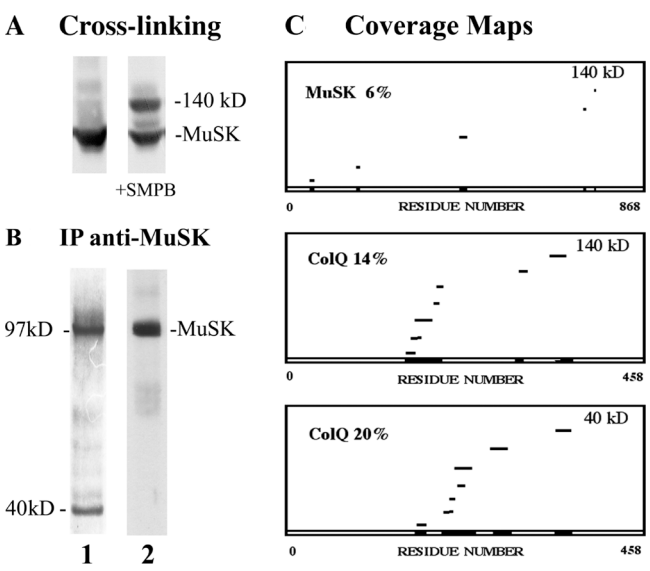

Figure 3. **MALDI-TOF mass spectrometry analysis of MuSK complex isolated from *Torpedo* AChR-rich membranes.** (A) Cross-linking experiment showing a major 140-kD MuSK cross-linked product in *Torpedo* AChR-rich membranes. After separation on SDS-PAGE, MuSK (97 kD) from control membranes (left lane) and from cross-linked membranes (right lane, +SMPB) were revealed by Western-blotting using anti-MuSK antibodies (Abs 2847). (B) Immunoprecipitation experiments performed on Triton X-100 extracts from uncross-linked *Torpedo* postsynaptic membranes with anti-MuSK antibodies. Lane 1 shows the presence of two polypeptides of relative MW 97 and 40 kD (silver staining after SDS-PAGE). Lane 2 shows Western blots performed with anti-MuSK showing that the 97-kD polypeptide corresponds to MuSK. (C) MALDI-TOF mass spectrometry analysis of the 140-kD cross-link product and the 40-kD polypeptide. Coverage maps are shown. Coverages of 6% with rat MuSK (top) and of 14% with rat AChE-associated collagen (ColQ) were obtained from the 140-kD cross-link product. On the 19 experimental tryptic peptides identified, seven matched with rat ColQ (182-190, 282-292, 158-169, 170-181, 155-169, 158-175, and 314-332). The matched peptides represent 79/458 residues of ColQ (14%). For the 40-kD polypeptide, a coverage of 20% was found with rat AChE-associated collagen. On the 15 experimental tryptic peptides identified, seven matched with rat ColQ (185-196, 200-211, 188-199, 155-169, 314-332, 197-217, and 238-261). The matched peptides represent 106/458 residues of ColQ (20%).

Western blotting. Among them, two major cross-linked products of 125 and 140 kD were detected in addition to uncross-linked MuSK (97 kD; Fig. 3 A). In the absence of cross-link, immunopurification experiments revealed a 40-kD polypeptide that copurified with MuSK (Fig. 3 B). The 140-kD cross-linked product as well as the 40-kD polypeptide were analyzed by matrix-assisted laser desorption ionization-time of flight (MALDI-TOF) mass spectrometry after tryptic digestion as described previously (Strochlic et al., 2001; Fig. 3 C). In the 140-kD cross-linked product, a sequence coverage of 6% was obtained with rat MuSK with a probability score of 10^{-4}. A manual comparison between the peptides from *Torpedo* and mammalian MuSK led to a higher coverage between the two sequences (13%), coherent with the overall 70% amino acid identity between *Torpedo* and rat MuSK sequences. In addition to MuSK, MALDI-TOF mass spectrometry analysis revealed the presence of ColQ with a coverage of 14%, and an estimated Z score

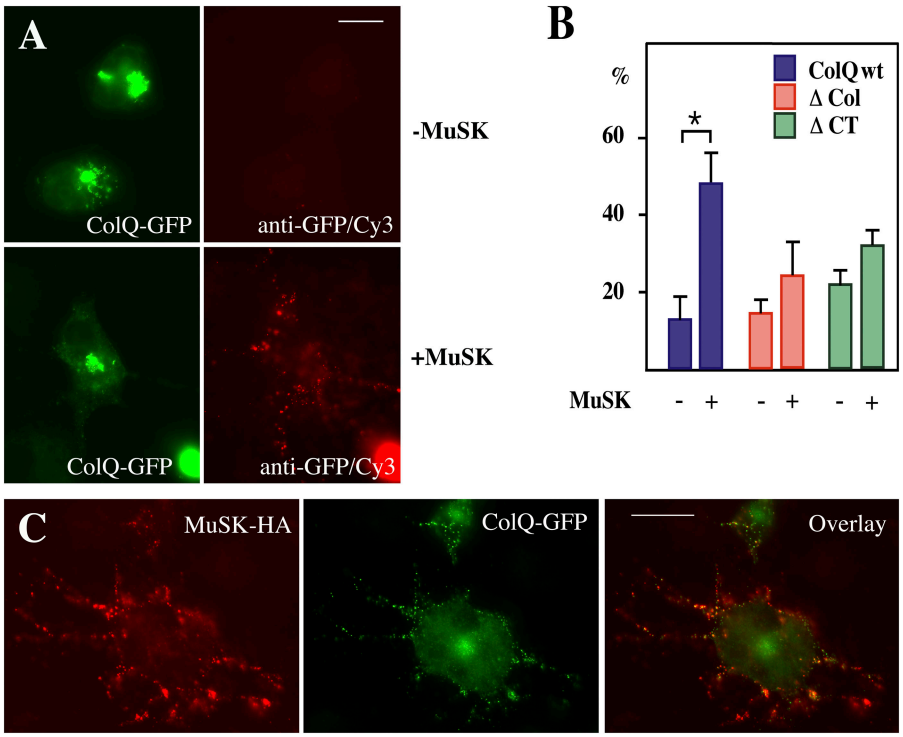

Figure 4. **ColQ-GFP and MuSK-HA co-aggregate at the cell surface in transfected COS-7 cells.** (A) Cell surface expression in COS-7 cells transfected with cDNAs encoding wt ColQ-GFP alone (−MuSK) or cotransfected with cDNAs encoding ColQ-GFP and MuSK-HA (+MuSK) was monitored by indirect immunofluorescence performed on unpermeabilized cells. Cell surface detection of ColQ expression was achieved using an additional anti-GFP antibody revealed with CY3-conjugated antibody. Then, the cell surface labeling appeared in red whereas intracellular ColQ-GFP was in green. In the absence of MuSK, only a few cells expressing ColQ-GFP intracellularly exhibited surface labeling, usually in clusters (B, ≈10%). In contrast, ≈50% of ColQ-GFP–positive cells expressed numerous surface clusters of ColQ-GFP in presence of MuSK. (B) Quantification of the immunolocalization data for wt ColQ and ColQ mutants. Ordinate indicates the percentage of cells in which surface clusters of wt ColQ, ΔCol, and ΔCt were detected ($n = 4$). Asterisk indicates statistical significance ($P < 0.05$) for the data shown in A. No significant increases in cells expressing ΔCol-GFP or ΔCt-GFP after MuSK transfection were observed. Means ± SEM are shown. (C) Wt ColQ-GFP and MuSK-HA co-distributed in aggregates at the cell surface as revealed by indirect immunofluorescence experiments performed on unpermeabilized cells. Enhancement of ColQ labeling at the cell surface was achieved using an additional anti-GFP antibody revealed with a FITC-conjugated goat anti mouse antibody. An anti-HA antibody was used to reveal MuSK followed by Cy3-conjugated goat anti–rabbit antibody. Note that colors are inverted for ColQ detection at the cell surface in A and C. Bars, 10 μm.

equals 1.95. MALDI-TOF mass spectrometry analysis of the 40-kD polypeptide revealed a coverage of 20% with ColQ, and an estimated Z score equals 1.67. These coverages were in agreement with the extensive sequence homology between the primary structures of collagenic tails from *Torpedo* and mammals (Krejci et al., 1991, 1997). Moreover, immunoprecipitation experiments performed in postsynaptic membranes from *Torpedo* electric tissue with anti-MuSK antibodies revealed that the catalytic subunit of AChE was also present in the MuSK complex (unpublished data). Together, our data indicate that MuSK is a membrane receptor for the collagenic tail of AChE. Therefore, we hypothetized that MuSK participates in AChE clustering on cell surface.

MuSK and ColQ form a complex in transfected COS-7 cells

COS-7 cells do not produce ColQ or MuSK. We first tested whether MuSK influences the cell surface expression of ColQ. Because most of ColQ-GFP appears in intracellular compartments (see also infra in Fig. 5), we specifically visualized extracellular ColQ. Unpermeabilized COS-7 cells transfected with rat cDNA encoding ColQ-GFP were immunolabeled with anti-GFP antibodies revealed with Cy3-conjugated antibodies (red fluorescence). In these conditions, the red fluorescence reveals the presence of ColQ exposed at the cell surface (Fig. 4 A). In COS-7 cells transfected with wt ColQ-GFP alone, only a limited number of cells expressing ColQ-GFP intracellularly also expressed it at the cell surface (≈10%, Fig. 4, A and B). In contrast, when cells were cotransfected with MuSK-HA and wt ColQ-GFP, ≈50% of the ColQ-GFP–positive cells expressed ColQ clusters at the cell surface (Fig. 4, A and B). It should be noted that ColQ clusters per cell were also increased in the presence of MuSK (unpublished data). In contrast, the ΔCol-GFP and ΔCt-GFP mutants were poorly accumulated at the cell surface, as shown by the lower percentage of cells exhibiting clusters in the presence of MuSK (Fig. 4 B). To further investigate the participation of MuSK in the surface localization of ColQ, we studied the co-distribution of the two molecules using double fluorescence experiments in which MuSK-HA was revealed with Cy3-conjugated anti-HA antibodies and ColQ-GFP with FITC-conjugated anti-GFP antibodies to enhance the detection of ColQ-GFP in unpermeabilized cells. Fig. 4 C shows that the majority of ColQ co-distributed with MuSK-HA within clusters at the cell surface. Thus, ColQ is retained more efficiently at the cell surface in the presence of MuSK and this property requires the collagen and the COOH terminus domains of ColQ.

To define which domain of ColQ is involved in the interaction with MuSK, we performed immunoprecipitation experiments with anti-MuSK antibodies (cyt-MuSK) 24 h after transient cotransfection of COS-7 cells. COS cells were transfected with cDNAs encoding MuSK-myc and either wt ColQ-GFP or several deleted or mutated forms of ColQ, i.e., ΔCt-GFP, ΔCol-GFP, or Y431S-GFP. As revealed by Western blotting, MuSK-myc and wt ColQ-GFP were detected in immunoprecipitates with myc and GFP antibodies, respec-

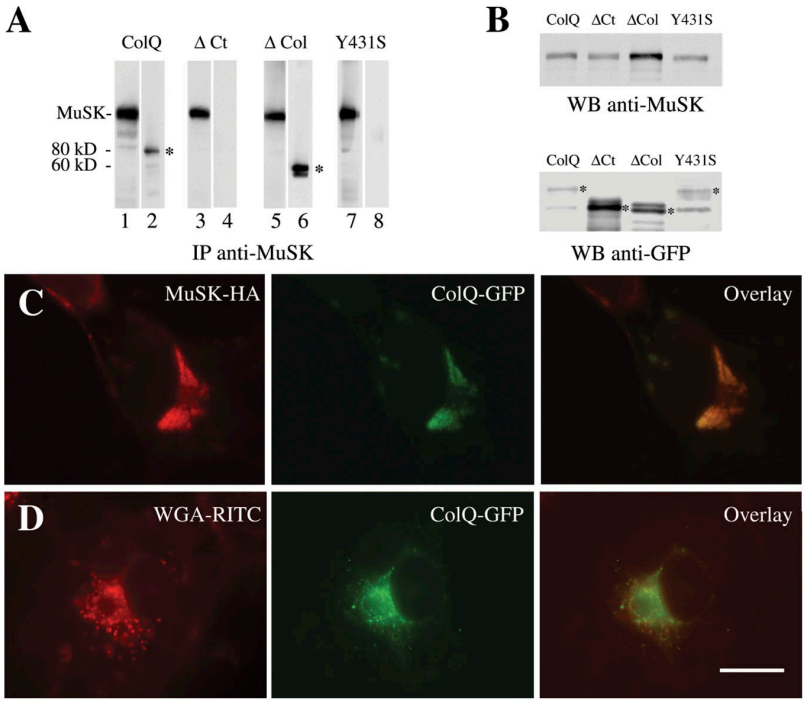

Figure 5. **ColQ-GFP and MuSK-myc coimmunoprecipitate in COS cells.** (A) Coimmunoprecipitation experiments were performed after cotransfection of COS-7 cells with constructs encoding wt ColQ-GFP or several deleted forms of ColQ-GFP (ΔCol and ΔCt) or of a point mutation in ColQ COOH-terminal domain (Y431S) together with MuSK-myc. Immunoprecipitates were done with anti-MuSK antibodies and revealed by Western blotting using anti-myc and anti-GFP antibodies. Lanes 1, 3, 5, and 7 indicate anti-myc; lanes 2, 4, 6, and 8 indicate anti-GFP. Only wt ColQ-GFP (80 kD; lane 2, asterisk) and the truncated ΔCol-GFP form (60 kD; lane 6, asterisk) coimmunoprecipitated with MuSK. (B) The levels of expression of MuSK (WB anti-MuSK) and the various forms of ColQ (WB anti-GFP) were shown by Western blotting performed on cell lysates from the same experiment as shown in A. Note that ΔCt and ΔCol are particularly highly expressed. Asterisks indicate the position of the main ColQ polypeptides (apparent MW 79 kD, 72 kD, 58 kD, and 78 kD for ColQ wt, ΔCt, ΔCol, and Y431S, respectively). (C) Colocalization of wt ColQ-GFP and MuSK-HA within intracellular compartments of transfected COS-7 cells. (D) ColQ-GFP labeling coincided to a large extent with the labeling of *N*-acetylglucosamine revealed by the lectin WGA, a marker of the Golgi compartment. Bar, 10 μm.

tively (Fig. 5 A, lanes 1 and 2). MuSK-myc and ColQ-GFP deleted from its collagenic domain (ΔCol-GFP) also coimmunoprecipitated (Fig. 5 A, lanes 5 and 6). Conversely, ΔCt-GFP or Y431S-GFP was not recovered in immunoprecipitates (Fig. 5 A, lanes 3 and 4, and lanes 7 and 8, respectively). In these experiments, we have verified that both MuSK-myc (Fig. 5 B, WB anti-MuSK) and ColQ-GFP mutants were expressed in transfected cells (Fig. 5 B, WB anti-GFP). In particular, ΔCt-GFP and ΔCol-GFP constructs were expressed at a high level strengthening the results of the immunoprecipitation experiments (Fig. 5 A, lanes 3 and 4, and lanes 5 and 6, respectively). These data demonstrate that the noncollagenous COOH-terminal domain of ColQ contains a binding site for MuSK whereas the collagen domain of ColQ is not involved in MuSK interaction. Large intracellular pools of transfected MuSK-HA and ColQ-GFP were detected when cells were permeabilized before immunolabeling. Both ColQ-GFP and MuSK-HA co-distributed within intracellular compartments (Fig. 5 C), likely of the exocytic pathway, as shown by the co-labeling of these compartments by the lectin WGA-RITC, a marker of Golgi compartment (Fig. 5 D). Thus, the immunoprecipitation experiments shown in Fig. 5 A partly reflect intracellular association.

ColQ-GFP, MuSK-HA, and perlecan co-distribute in transfected COS cells

We observed that the truncated ΔCol mutant lacking the collagen domain containing the two HBS, though coimmunoprecipitating with MuSK by its COOH-terminal domain, was less efficiently accumulated at the cell surface of MuSK cotransfected COS-7 cells compared with wt ColQ (Fig. 4 B). Similarly, the ΔCt mutant lacking the COOH-terminal domain involved in the interaction with MuSK was also less efficiently accumulated in the MuSK cotransfected cells (Fig. 4 B). Thus, the collagen and the COOH-terminal domains are both required for cell surface localization of ColQ. To deter-

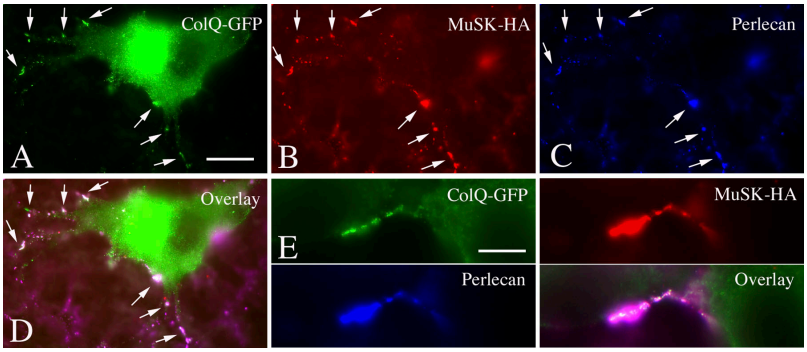

Figure 6. **ColQ-GFP, MuSK, and perlecan co-distribute in transfected COS-7 cells.** COS-7 cells were cotransfected with cDNA encoding ColQ-GFP and MuSK-HA, and visualized by triple indirect immunofluorescence performed on unpermeabilized cells. ColQ-GFP labeling exposed at the cell surface was amplified using an additional anti-GFP antibody revealed with a FITC-conjugated goat anti–mouse antibody (see Materials and methods). Triple labeling imaging showing that ColQ-GFP (A), MuSK-HA (B), and perlecan (Cy5 fluorescence in false blue color in C) colocalized within clusters at the cell surface. The white color in the overlay (D) corresponded to the superimposition of the three proteins: green, ColQ-GFP; red, MuSK-HA; blue, perlecan (arrows). Details of the cell surface labeling of these three proteins are shown in E. Bars: (A) 10 μm; (E) 3 μm.

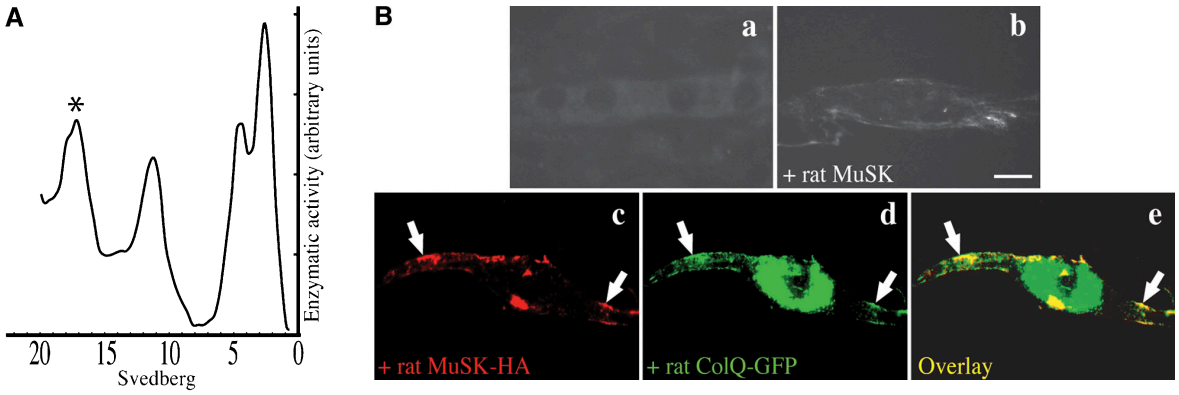

Figure 7. **MuSK restores the formation of AChE clusters in MuSK-deficient MTs.** (A) Sedimentation analysis of the molecular forms produced by MuSK-deficient cells revealed that these cells produced A_{12} forms indicated by the asterisk in the sedimentation profile. (B) MTs in culture were labeled with antibodies to either AChE (a and b) or to MuSK-HA or to ColQ-GFP (c and d). No AChE (a) clusters were detected in MuSK-deficient MTs. AChE clusters were restored when MuSK-deficient MTs were transfected with rat MuSK (b). Clusters of MuSK-HA (c) and ColQ-GFP (d) colocalized in MuSK-deficient cells cotransfected with MuSK-HA and ColQ-GFP as shown on the overlay picture (e). Arrows show colocalizations of ColQ-GFP and MuSK-HA. Bar, 20 μm.

mine whether the aggregates containing ColQ and MuSK also contained perlecan, we looked for the presence of perlecan in these aggregates in triple immunofluorescence experiments. We first verified that cultured COS-7 cells express perlecan at the cell surface (unpublished data). Triple labeling experiments were performed in COS-7 cells doubly transfected with ColQ-GFP and MuSK-HA. Strikingly, ColQ-GFP clusters mostly co-distributed with MuSK-HA and perlecan (Fig. 6, A–E). In rare occurrence, ColQ-GFP clusters not associated with MuSK/perlecan were observed. Together, with the previous data which emphasize the requirement of the two HBS and COOH-terminal domain of ColQ in the anchoring of AChE at the cell surface, these experiment suggest that a ternary complex comprising ColQ, MuSK, and perlecan participates to the mechanism of AChE accumulation.

MuSK expression restores ColQ clusters in MuSK-deficient MTs

Because no cluster of AChE are detected in MuSK deficient MTs (DeChiara et al., 1996), we wondered whether these cells produce A forms. As shown by sedimentation analysis, they do express these molecular forms (Fig. 7 A). No AChE clusters could be seen in MuSK-deficient MTs (Fig. 7 B, a) but when these cells were transfected with a rat MuSK cDNA, MuSK expression rescued the ability of these MTs to form spontaneous AChE clusters (Fig. 7 B, b). When MuSK-HA and ColQ-GFP were cotransfected in MuSK-deficient MTs, most of these two proteins were shown to colocalize (Fig. 7 B, c–e).

Discussion

The localization of AChE at synaptic sites in muscle relies on the presence of a structural subunit, ColQ. Various observations prompted us to seek another direct partner in addition to perlecan in the clustering of AChE at the NMJ. Here, we report that the hetero-oligomer AChE-ColQ is accumulated in clusters through a complex mechanism that involves three sites, the two HBS contained in the collagen domain and the COOH terminus of ColQ. We demonstrate that none of the three sites are dispensable for accumulating ColQ at the cell surface in MTs or COS-7 cells. We provide the first evidence that ColQ binds MuSK through its COOH-terminal domain.

AChE clusters form with muscle cell late differentiation

Previous works have shown that a number of synaptic proteins including AChE, are up-regulated upon MT formation (Chakkalakal and Jasmin, 2003). This process also applies to ColQ. In our mouse muscle cell cultures, AChE clusters appear at the time of muscle contraction. This is consistent with the absence of AChE clusters in C2C12 mouse muscle cell line that does not spontaneously contract (unpublished data). It has been reported that spontaneous contraction of rat muscle cells grown in neuron-free primary cultures stimulates the synthesis of AChE subunits, a process that can be mimicked by the addition of calcium in the absence of contraction (Rubin, 1985). Because calcium has been shown to stabilize AChE mRNAs (Luo et al., 1994), we may then hypothesize that spontaneous muscle contraction induces a large increase in intracellular calcium concentration which, in turn, leads to an increase in the number of AChE subunits synthesized. As a consequence, AChE subunits would fill the three strands of ColQ and the saturated hetero-oligomers would then become detectable within clusters. Furthermore, contraction correlates with a large increase in ColQ mRNAs levels, a process that could also induce the production of AChE-collagen–tailed forms. However, we cannot exclude that the formation of clusters are generated from a late differentiation process occurring with muscle contraction.

Distinct sites located within ColQ are necessary for the formation of AChE clusters

Previous observations from ColQ-deficient mouse have shown in vivo that the formation of AChE synaptic clusters relies on the presence of ColQ (Feng et al., 1999). ColQ-deficient myogenic cells are devoided of AChE clusters, and the transfection of ColQ in these cells restores the presence

of clusters confirming the in vivo results. AChE accumulation in the basal lamina does require ColQ.

Using a series of constructs in which each one of the two HBS or the COOH terminus domain of ColQ was mutated, we demonstrated that AChE accumulation requires the presence of the three sites in MTs and in COS-7 cells. Previous data have demonstrated that the affinity of ColQ for heparin resides exclusively in two HBS contained in the collagen domain and that these two sites have different biochemical properties (Deprez et al., 2003). The biochemical specificity of these sites is strengthened by our data showing that the two HBS are not redundant in clustering ColQ. Because the ColQ COOH terminus domain has no affinity for heparin, it excludes the possibility that this domain interacts with HSPGs.

Our results explain observations made in patients bearing mutations in the COOH terminus domain of ColQ associated with a congenital end plate AChE deficiency (Ohno et al., 2000). For most of these mutations, tetramers of catalytic subunits and ColQ associate but A forms do not accumulate in the NMJ. In the case of the point mutation Y431S that we have reproduced in the rat ColQ cDNA for this work, trace amounts of AChE are detected at the end plate of intercostal muscles in patients although normal levels of A forms were produced (Donger et al., 1998). Thus, this mutation prevents or severely hinders the accumulation of AChE into the synaptic basal lamina. The present data show that this single point mutation in the COOH terminus domain of ColQ is critical for the synaptic accumulation of AChE.

ColQ binds MuSK trough its COOH terminus

Several mouse mutants are characterized by an absence or a reduction in the number of AChE clusters at the synapse. These mutants can be classified in three groups: (1) mutants of the basal lamina proteins such as perlecan; (2) mutants of intrinsic membrane proteins such as dystroglycan and MuSK; and (3) mutants of extrinsic or cytoskeletal proteins such as rapsyn and α-syntrophin (for review see Sanes and Lichtman, 2001). For most of these mutants, the absence of AChE clusters can be explained by a perturbation of the ColQ–perlecan-DG scaffold. The perturbation results either from the absence of one of the ColQ partners in the scaffold or from the absence of a key component involved in the assembly of the scaffold, i.e., MuSK. Alternatively, ColQ COOH terminus could directly bind to MuSK.

Here, we provide compelling biochemical and cytological evidences that ColQ binds MuSK. (a) Cross-linking experiments argue in favor of a direct link between MuSK and ColQ. (b) Mutants of ColQ bearing a deletion or the point mutation Y431S in the COOH terminus domain are expressed but cannot be immunoprecipitated together with MuSK from transfected COS-7 cells. Thus, the AChE deficiency observed in patients bearing the Y431S mutation can now be explained by the lack of interaction between ColQ and MuSK. (c) AChE clusters do not form in MuSK-deficient cells although both AChE and ColQ are expressed in these cells. (d) MuSK restores the presence of AChE clusters in MuSK-deficient cells. (e) ColQ colocalizes with MuSK in clusters. Although perlecan has been suggested to be the unique acceptor molecule for AChE-ColQ at the NMJ (Arikawa-Hirasawa et al., 2002), our observations show that MuSK also binds ColQ and is necessary for AChE-ColQ accumulation. Together, the present data provide a simple mechanism for the accumulation of collagen-tailed forms of AChE at synaptic sites. Whereas perlecan is rather widely distributed along the entire muscle basal lamina, MuSK is strictly accumulated at the synapse. Therefore, the collagen-tailed forms of AChE can only be accumulated at the synapse where its two binding partners, perlecan and MuSK coexist. This is corroborated by previous observations showing that MuSK injected ectopically in soleus muscle induces the formation of AChE clusters (Sander et al., 2001). Indeed, in extrasynaptic domains of this muscle, perlecan, ColQ, and AChE are present and the injection of MuSK complements the set of molecules necessary for AChE cluster formation.

At the NMJ, MuSK is mostly observed at the crests of the postsynaptic membrane folds (Trinidad et al., 2000). This localization does not completely overlap AChE distribution at the synapse, which is distributed at the crests and the depths of the folds (Anglister et al., 1998; unpublished data). One explanation would be that MuSK is also present in the depths of the folds but at a lower level compared with the top of the folds, still compatible with the formation of the complex. An alternative hypothesis is that the COOH terminus domain of ColQ could bind another component present in the depths of the folds.

In this work, we show that ColQ, in addition to nerve-derived agrin, binds MuSK. In ColQ-deficient MTs in culture, the number of AChR aggregates increased when agrin was applied to the culture (unpublished data). Because ColQ is dispensable for agrin-induced AChR clustering, it is not the coreceptor for agrin. However, we cannot exclude that ColQ could modulate the effect of agrin on MuSK. Accordingly, Hopf and Hoch (1997) have suggested that in addition to agrin, a component sensitive to heparin binds MuSK and modulates its activity.

Clusters of AChE and AChR form independently

An interesting conclusion drawn from the present observations is that the formation of AChR and AChE clusters both relies on MuSK but through independent mechanisms. Whereas clusters of ACh receptors form in response to a transduction pathway induced by agrin-activated MuSK, AChE clusters form by structural interaction between ColQ and MuSK. Whether the interaction of ColQ with MuSK is strictly structural or could also activate a downstream pathway remains an open question.

MuSK: a central piece in the assembly of AChE clusters at the NMJ

In conclusion, the data reported here have focused on two classes of binding sites in ColQ which are required in the mechanism of AChE accumulation, pointing to the direct interaction of ColQ with perlecan and MuSK. Indeed, the three proteins form co-clusters in transfected COS cells. The present data suggest that a ternary complex involving MuSK and perlecan is responsible for the anchoring of AChE at the NMJ. As presented in our model (Fig. 8), a dual mechanism involving two different classes of binding sites is required for

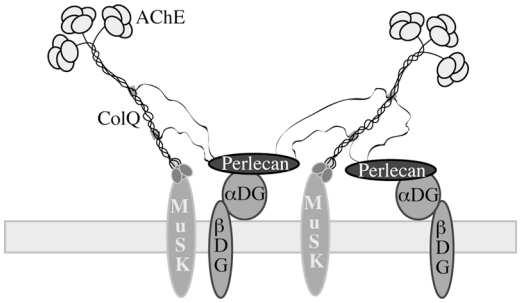

Figure 8. **Model illustrating the dual mechanism by which the A forms of AChE are accumulated at synaptic sites.** The two types of interactions between (a) the COOH terminus of ColQ and MuSK, and (b) the two HBS (gray boxes) in the collagen domain of ColQ and perlecan are shown. The interaction of perlecan and dystroglycan (αDG and βDG) is also represented. This model accounts for the accumulation of AChE in the synaptic basal lamina enriched in perlecandystroglycan and for its precise localization at postsynaptic sites via MuSK.

accumulating the enzyme in the synaptic cleft: one through the postsynaptic receptor MuSK conferring synaptic localization, and another through interactions with the HSPG, perlecan. We can hypothesize that these multiple interactions on ColQ are necessary for anchoring such a large molecule in the synaptic cleft.

Materials and methods

Antibodies and reagents

Polyclonal 2847 anti-*Torpedo* MuSK antibodies were a gift from S. Burden (Skirball Institute of Biomolecular Medicine, New York, NY; Watty et al., 2000). Polyclonal MuSK antibodies raised against the cytoplasmic domain of rat MuSK (cyt-MuSK) were a gift from W. Hoch (University of Houston, Houston, TX; Hopf and Hoch, 1998). Rabbit polyclonal anti-HA, chicken polyclonal anti-HA, mouse monoclonal anti-Myc, and monoclonal anti-GFP antibodies were purchased from Santa Cruz Biotechnology, Inc., Invitrogen, ICL, and Roche Molecular Biochemicals, respectively. Rabbit polyclonal antibodies directed against the COOH terminus domain (domain V) of perlecan were a gift from R. Timpl (Max-Planck Institute, Martinsried, Germany). A63 is a polyclonal rat anti-AChE raised in rabbit (Marsh et al., 1984). Goat CY3-conjugated polyclonal anti–chicken and donkey CY5-conjugated polyclonal rabbit antibodies were purchased from Abcam and Jackson ImmunoResearch Laboratories, respectively. RITC-conjugated WGA was purchased from Sigma-Aldrich.

Constructs

The rat $AChE_T$ and ColQ1a clones have been described previously (Legay et al., 1993; Krejci et al., 1999). A GFP tag was introduced 5′ from the PRAD exon in the ColQ-GFP construct. ColQ mutants ΔCt, ΔCol, N−/C+, N+/C−, and N−/C− have been described previously (Deprez et al., 2003). ColQ Y431S is a ColQ construct in which we have reproduced the human Y431S mutation by mutagenesis. MuSK cDNA clone, MuSK-HA, and MuSK-myc constructs were gifts from W. Hoch (Hopf and Hoch, 1997). The tags HA and myc were introduced at the NH_2 and COOH terminus, respectively. The MuSK-GFP construct was a gift from V. Witzemann (Max-Planck Institute, Martinsried, Germany; Sander et al., 2001).

Real-time RT-PCR assay

Total RNA was isolated using the RNeasy protect mini-kit (QIAGEN). 0.5 μg of purified RNAs were reversed transcribed using 500 ng of oligodT primers and the superscript II RNaseH kit (Invitrogen). RT reactions were performed three times on each RNA and the PCR reaction was repeated three times from each RT. Specific pairs of primers were as follows. F and R referred to the forward and reverse primers, respectively. Primers for $AChE_T$ cDNAs were 5′-GCAATATGTGAGCCTGAACCTG-3′ ($AChE_T$F) and 5′-TCACAGGTCTGAGCAGCGTTC-3′ ($AChE_T$R). Primers for ColQ1 and ColQ1a cDNAs were: 5′-CAACTCTTCTTCTGCTCCATCG-3′ (ColQ1F), 5′-CTTTGGTCCTGTCTTGCCAG-3′ (ColQ1R), and 5′-ACGGGTCCATCATTCACTCATC-3′ (ColQ1aF). The ColQ1aR was identical to ColQ1R. GADPH cDNAs were used as internal standards. Primers for GAPDH were: 5′-ATGAATACGGCTACAGCA-3′ (GADPHF) and 5′-GCCCCTCCGTTATTATGG-3′ (GADPHR). Amplifications were performed in a light cycler (Roche Diagnostics) using the Quantitect SYBR Green PCR kit (QIAGEN). Denaturation and activation of the Hotstart polymerase were performed at 94°C for 14 min (1 cycle) followed by 50 cycles of denaturation, hybridization, and extension of 94°C for 10 s, 62°C for 27 s, and 72°C for 13 s. Standard linear curves were generated for each couple of primers using serial dilutions of the RT reaction. Quantifications were made from cycle threshold (C_T) within these standard curves. Relative expression levels of $AChE_T$, ColQ1, and ColQ1a mRNAs were determined according to GAPDH levels as an internal control.

Muscle cell cultures, transfections, immunocytochemistry, and molecular form analysis

Two muscle cell lines were generated from wt and $ColQ^{-/-}$: H-2kb-tsA58 week-old mice. These mice bear a temperature-sensitive SV40 T antigene under the control of an interferon-inducible promoter (Jat et al., 1991). Limb muscles of the transgenic mice were dissociated and the cell lines were established according to the protocol described in Herbst and Burden (2000). Myoblast cells were cultured at 33°C in 8.5% CO_2 and in DME supplemented with 2 mM glutamine, 2% penicillin/streptomycin (5,000 U), and 20 U/ml of γ-interferon (Roche Diagnostics). All the culture medium reagents were purchased from Invitrogen Life Technologies. Cells were differentiated into MTs in the same medium without interferon.

For expression assays, cells were cultured on plates coated with Matrigel (Becton Dickinson) and were transfected as 80% confluent myoblasts with ExGen 500 (Euromedex). Cells were induced to fuse one day after transfection. Using this protocol, 50–70% of the cells expressed the transfected cDNAs.

Immunostaining was performed either 5–7 d after transfection or 15–20 d after transfection for contracting MTs. MTs were fixed for 10 min in 2% PFA-phosphate buffer. In some experiments, cells were permeabilized with 0.5% Triton X-100 for 5 min before proceeding to incubations with antibodies. Before the reaction with antibodies, non specific binding was blocked using the block reagent (DakoCytomation) for 10 min. Cells were first incubated with the primary antibody for 1 h at RT and washed in Glycine-BSA (0.15%:0.15%) buffer and incubated with a fluorochrome-conjugated secondary antibody for 30 min. All of the fluorochrome-conjugated antibodies were purchased from Jackson ImmunoResearch Laboratories and used at a 150 mM concentration. When double labeling was performed, the two primary antibodies were sequentially used.

AChE was visualized with the polyclonal A63 antibody raised against rat AChE (Marsh et al., 1984). Proteins tagged with GFP were visualized using GFP antibodies (1:200; Roche Diagnostics). MuSK tagged with the HA epitope was revealed with rat monoclonal anti-HA (1:1,000; Roche Diagnostics). AChRs were visualized with α-bungarotoxin conjugated either to Alexa 488 or to rhodamine (Molecular Probes). Micrographs were taken with a DMR microscope (Leica) equipped with an NA1.4 63× Plan Apo objective. Images were captured with a Micro MaX cooled CDD camera (Princeton Instruments, Inc.) driven by Meta View Imaging system (Universal Imaging Corp.). Figures were organized using Adobe Photoshop v6.0.

Analysis of the molecular forms was done by sucrose density gradient centrifugation as described previously (Bon et al., 1997). For analysis of the molecular forms produced by ColQ-deficient cells cotransfected with AChE and the wt or mutant ColQ constructs, the procedure was the following. Transfected cells were cultured in differentiation medium for 144 h and a first aliquot was taken at that time for sedimentation analysis. The same transfected cells were then treated with heparin (1 mg/ml in the culture medium; Sigma-Aldrich) for 24 h and a second aliquot was analyzed at the end of this treatment.

COS-7 cell culture, transfections, and immunofluorescence

For transfection experiments, COS-7 cells (purchased from American Type Culture Collection) cultured in DME were grown to 70% confluence on coverslips and transfected using FuGene 6 (Roche Diagnostics). Immunoprecipitation and immunofluorescence analyses were performed 48 h later. For indirect immunofluorescence, cells were rinsed in PBS at 37°C, blocked in PBS, BSA 1%, goat serum 0.5% for 20 min at RT, and incubated with primary antibodies without permeabilization of the cells to detect cell surface ColQ-GFP or MuSK-HA. For double fluorescence, monoclonal anti-GFP antibodies (1:20) and rabbit polyclonal anti-HA (1:500) used as primary antibodies were revealed with goat FITC-conjugated anti–

mouse antibodies (1:200) or Cy3-conjugated anti–rabbit (1:100), respectively. For triple fluorescence analyses, monoclonal anti-GFP antibodies (1:20), chicken polyclonal anti-HA (1:100) and rabbit polyclonal antiperlecan antibodies (1:50) used as primary antibodies were revealed with goat FITC-conjugated anti–mouse (1:200), Cy3-conjugated anti–chicken (1:100), and Cy5-conjugated anti–rabbit antibodies (1:200), respectively. In another series of experiments, to detect intracellular as well as cell surface labeling, transfected cells were permeabilized with Triton X-100 0.1% after fixation in 3% PFA and before incubation with either rabbit polyclonal anti-HA antibodies (1:500), followed by goat Cy3-conjugated anti–rabbit (1:100) or WGA-RITC (Sigma-Aldrich; 1:400). For double- and triple-fluorescence pictures, controls confirmed that no bleedthrough was detectable under the conditions used (filter L5 for fluorescein, TX for CY3, or XF 47 for CY5). CY5 fluorescence was artificially colored in blue. Micrographs were taken as described above. For quantification of cells expressing wt ColQ or mutants ColQ ΔCt-GFP or ΔCol-GFP at the cell surface, we counted the number of cells expressing Cy3-labeled ColQ-GFP or ΔCt-GFP or ΔCol-GFP at the surface versus cells expressing intracellular wt ColQ-GFP or ΔCt-GFP or ΔCol-GFP. For each experiment ~150 GFP-positive cells were counted using a 40× objective.

Means reported in Fig. 4 were compared by analysis of variance. The equal variance test is significant with $P < 0.05$. Pair wise multiple comparisons were made with *t* test.

Immunoprecipitation of MuSK-ColQ complexes in COS-7 cells

Culture dishes of 70% confluent COS-7 cells transfected with ColQ-GFP or mutants ΔCt-GFP, ΔCol-GFP, or Y431S and MuSK-myc were harvested in a lysis buffer (50 mM Tris, 150 mM NaCl, 2 mM EDTA, 2 mM orthovanadate, 1% Triton X-100) and 0.3 mM PMSF (Sigma-Aldrich) and antiproteases (1 μg/ml leupeptin, 1 μg/ml pepstatin, and 1 μg/ml aprotinin), pH 7.5, for 30 min at 4°C. Immunoprecipitation were performed on 1 ml of cell lysates incubated with 3 μg of anti–cyt-MuSK antibodies. Immunocomplexes were precipitated with protein A Sepharose according to the manufacturer's instructions (Amersham Biosciences) for 3 h at 4°C. Immunoprecipitates were then washed in lysis buffers, resuspended in 1× SDS sample buffer, resolved by 10% SDS-PAGE, and analyzed by Western blotting using anti-myc (1:1,000) and anti-GFP (1:200) antibodies. Aliquots from cell lysates were also used for detection of the levels of expression of MuSK and ColQ polypeptides by Western blotting.

Cross-linking experiments

Cross-linking experiments in *Torpedo* AChR-rich membranes (4 mg proteins/ml) were performed according to Burden et al. (1983) using succinimidyl 4(p-maleimidophenyl)-butyrate as described in Strochlic et al. (2001). The detection of MuSK in the cross-link products was subsequently achieved by Western blotting using anti–Cyt-MuSK (1:200) or 2847 antibodies (1:2,000) after separation of the proteins on 10% SDS-PAGE.

SDS-PAGE and Western blots

Samples were run on 10% SDS-PAGE according to Laemmli (1970) and electrotransferred to nitrocellulose membranes (Schleicher & Schuell). Western blots were performed as described previously (Cartaud et al., 1998) and revealed using ECL (Amersham Biosciences).

Immunopurification of the MuSK complex and MALDI-TOF mass spectrometry

Immunoprecipitation of the MuSK complex and MALDI-TOF spectrometry from fresh *Torpedo* electrocyte were performed as described in Strochlic et al. (2001).

We thank S. Burden for generous gifts of the MuSK-deficient cell line and anti-MuSK antibody, V. Labas and J. Rossier for mass spectrometry analysis, W. Hoch for MuSK cDNAs and anti-MuSK antibody, R. Timpl for anti-perlecan antibody, and V. Witzemann for MuSK-GFP construct. We also thank M. Recouvreur for expert technical assistance with cell cultures, C. Chamot for confocal microscopy, and A. Baulig for statistical analyses. We also thank Dr. Paola Deprez for helpful discussions. Part of this work has been presented at the 42nd Annual Meeting of the American Society for Cell Biology meeting in San Francisco, CA, on December 14–18, 2002 (Legay et al., 2002. *Mol. Biol. Cell*. 13:394a–395a).

This work was funded by the Centre National de la Recherche Scientifique, the Association Française contre les Myopathies (to J. Cartaud and C. Legay), the Ecole Normale Supérieure, and Universities Paris 6 and Paris 7. The authors declare they have no competing financial interests.

Note added in proof. While this paper was being reviewed, the groups of Rotundo and Engel also presented evidence that the two heparin-binding sites and the COOH terminus domain of ColQ are required for AChE accumulation (Kimbell, L.M., K. Ohno, A.G. Engel, and R.L. Rotundo. 2004. *J. Biol. Chem*. 279:10997–11005).

Submitted: 10 December 2003
Accepted: 19 April 2004

References

Anglister, L., J. Eichler, M. Szabo, B. Haesaert, and M.M. Salpeter. 1998. ^{125}I-labeled fasciculin 2: a new tool for quantitation of acetylcholinesterase densities at synaptic sites by EM-autoradiography. *J. Neurosci. Methods.* 81:63–71.

Arikawa-Hirasawa, E., S.G. Rossi, R.L. Rotundo, and Y. Yamada. 2002. Absence of acetylcholinesterase at the neuromuscular junctions of perlecan-null mice. *Nat. Neurosci.* 5:119–123.

Bon, S., F. Coussen, and J. Massoulié. 1997. Quaternary associations of acetylcholinesterase. II. The polyproline attachment domain of the collagen tail. *J. Biol. Chem.* 272:3016–3021.

Brandan, E., M. Maldonado, J. Garrido, and N.C. Inestrosa. 1985. Anchorage of collagen-tailed acetylcholinesterase to the extracellular matrix is mediated by heparan sulfate proteoglycans. *J. Cell Biol.* 101:985–992.

Burden, S.J., R.L. DePalma, and G.S. Gottesman. 1983. Crosslinking of proteins in acetylcholine receptor-rich membranes: association between the beta-subunit and the 43 kd subsynaptic protein. *Cell.* 35:687–692.

Burden, S.J. 2002. Building the vertebrate neuromuscular synapse. *J. Neurobiol.* 53:501–511.

Cartaud, A., S. Coutant, T.C. Petrucci, and J. Cartaud. 1998. Evidence for in situ and in vitro association between beta-dystroglycan and the subsynaptic 43K rapsyn protein. Consequence for acetylcholine receptor clustering at the synapse. *J. Biol. Chem.* 273:11321–11326.

Chakkalakal, J.V., and B.J. Jasmin. 2003. Localizing synaptic mRNAs at the neuromuscular junction: it takes more than transcription. *Bioessays.* 25:25–31.

DeChiara, T.M., D.C. Bowen, D.M. Valenzuela, M.V. Simmons, W.T. Poueymirou, S. Thomas, E. Kinetz, D.L. Compton, E. Rojas, J.S. Park, et al. 1996. The receptor tyrosine kinase MuSK is required for neuromuscular junction formation in vivo. *Cell.* 85:501–512.

Deprez, P.N., and N.C. Inestrosa. 1995. Two heparin-binding domains are present on the collagenic tail of asymmetric acetylcholinesterase. *J. Biol. Chem.* 270:11043–11046.

Deprez, P.N., N.C. Inestrosa, and E. Krejci. 2003. Two heparin-binding domains in the triple-helical domain of ColQ, the collagen tail subunit of synaptic acetylcholinesterase. *J. Biol. Chem.* 278:23233–23242.

Donger, C., E. Krejci, A.P. Serradell, B. Eymard, S. Bon, S. Nicole, D. Chateau, F. Gary, M. Fardeau, J. Massoulie, and P. Guicheney. 1998. Mutation in the human acetylcholinesterase-associated collagen gene, COLQ, is responsible for congenital myasthenic syndrome with end-plate acetylcholinesterase deficiency (Type Ic). *Am. J. Hum. Genet.* 63:967–975.

Engel, A.G., K. Ohno, and S.M. Sine. 2003. Sleuthing molecular targets for neurological diseases at the neuromuscular junction. *Nat. Rev. Neurosci.* 4:339–352.

Feng, G., E. Krejci, J. Molgo, J.M. Cunningham, J. Massoulie, and J.R. Sanes. 1999. Genetic analysis of collagen Q: roles in acetylcholinesterase and butyrylcholinesterase assembly and in synaptic structure and function. *J. Cell Biol.* 144:1349–1360.

Hall, Z.W., and R.B. Kelly. 1971. Enzymatic detachment of endplate acetylcholinesterase from muscle. *Nat. New Biol.* 232:62–63.

Herbst, R., and S.J. Burden. 2000. The juxtamembrane region of MuSK has a critical role in agrin-mediated signaling. *EMBO J.* 19:67–77 (published erratum in *EMBO J.* 2000. 19:1167).

Hopf, C., and W. Hoch. 1997. Heparin inhibits acetylcholine receptor aggregation at two distinct steps in the agrin-induced pathway. *Eur. J. Neurosci.* 9:1170–1177.

Hopf, C., and W. Hoch. 1998. Dimerization of the muscle-specific kinase induces tyrosine phosphorylation of acetylcholine receptors and their aggregation on the surface of myotubes. *J. Biol. Chem.* 273:6467–6473.

Jacobson, C., P.D. Cote, S.G. Rossi, R.L. Rotundo, and S. Carbonetto. 2001. The dystroglycan complex is necessary for stabilization of acetylcholine receptor clusters at neuromuscular junctions and formation of the synaptic basement membrane. *J. Cell Biol.* 152:435–450.

Jasmin, B.J., R.K. Lee, and R.L. Rotundo. 1993. Compartmentalization of acetylcholinesterase mRNA and enzyme at the vertebrate neuromuscular junction.

Neuron. 11:467–477.

Jat, P.S., M.D. Noble, P. Ataliotis, Y. Tanaka, N. Yannoutsos, L. Larsen, and D. Kioussis. 1991. Direct derivation of conditionally immortal cell lines from an H-2Kb-tsA58 transgenic mouse. *Proc. Natl. Acad. Sci. USA.* 88:5096–5100.

Krejci, E., F. Coussen, N. Duval, J.M. Chatel, C. Legay, M. Puype, J. Vandekerckhove, J. Cartaud, S. Bon, and J. Massoulié. 1991. Primary structure of a collagenic tail peptide of Torpedo acetylcholinesterase: co-expression with catalytic subunit induces the production of collagen-tailed forms in transfected cells. *EMBO J.* 10:1285–1293.

Krejci, E., S. Thomine, N. Boschetti, C. Legay, J. Sketelj, and J. Massoulié. 1997. The mammalian gene of acetylcholinesterase-associated collagen. *J. Biol. Chem.* 272:22840–22847.

Krejci, E., C. Legay, S. Thomine, J. Sketelj, and J. Massoulié. 1999. Differences in expression of acetylcholinesterase and collagen Q control the distribution and oligomerization of the collagen-tailed forms in fast and slow muscles. *J. Neurosci.* 19:10672–10679.

Laemmli, U.K. 1970. Cleavage of structural proteins during the assembly of the head of bacteriophage T4. *Nature.* 227:680–685.

Legay, C., S. Bon, P. Vernier, F. Coussen, and J. Massoulié. 1993. Cloning and expression of a rat acetylcholinesterase subunit: generation of multiple molecular forms and complementarity with a Torpedo collagenic subunit. *J. Neurochem.* 60:337–346.

Legay, C., M. Huchet, J. Massoulié, and J.P. Changeux. 1995. Developmental regulation of acetylcholinesterase transcripts in the mouse diaphragm: alternative splicing and focalization. *Eur. J. Neurosci.* 7:1803–1809.

Legay, C., F.A. Mankal, J. Massoulié, and B.J. Jasmin. 1999. Stability and secretion of acetylcholinesterase forms in skeletal muscle cells. *J. Neurosci.* 19: 8252–8259.

Legay, C. 2000. Why so many forms of acetylcholinesterase? *Microsc. Res. Tech.* 49: 56–72.

Luo, Z., M.E. Fuentes, and P. Taylor. 1994. Regulation of acetylcholinesterase mRNA stability by calcium during differentiation from myoblasts to myotubes. *J. Biol. Chem.* 269:27216–27223.

Marsh, D., J. Grassi, M. Vigny, and J. Massoulié. 1984. An immunological study of rat acetylcholinesterase: comparison with acetylcholinesterases from other vertebrates. *J. Neurochem.* 43:204–213.

McMahan, U.J., J.R. Sanes, and L.M. Marshall. 1978. Cholinesterase is associated with the basal lamina at the neuromuscular junction. *Nature.* 271:172–174.

Ohno, K., J. Brengman, A. Tsujino, and A.G. Engel. 1998. Human endplate acetylcholinesterase deficiency caused by mutations in the collagen-like tail subunit (ColQ) of the asymmetric enzyme. *Proc. Natl. Acad. Sci. USA.* 95: 9654–9659.

Ohno, K., A.G. Engel, J.M. Brengman, X.M. Shen, F. Heidenreich, A. Vincent, M. Milone, E. Tan, M. Demirci, P. Walsh, et al. 2000. The spectrum of mutations causing end-plate acetylcholinesterase deficiency. *Ann. Neurol.* 47:162–170 (published erratum in *Ann. Neurol.* 2000. 47:554).

Peng, H.B., H. Xie, S.G. Rossi, and R.L. Rotundo. 1999. Acetylcholinesterase clustering at the neuromuscular junction involves perlecan and dystroglycan. *J. Cell Biol.* 145:911–921.

Rossi, S.G., and R.L. Rotundo. 1996. Transient interactions between collagen-tailed acetylcholinesterase and sulfated proteoglycans prior to immobilization on the extracellular matrix. *J. Biol. Chem.* 271:1979–1987.

Rotundo, R.L., S.G. Rossi, and L. Anglister. 1997. Transplantation of quail collagen-tailed acetylcholinesterase molecules onto the frog neuromuscular synapse. *J. Cell Biol.* 136:367–374.

Rubin, L.L. 1985. Increases in muscle Ca^{2+} mediate changes in acetylcholinesterase and acetylcholine receptors caused by muscle contraction. *Proc. Natl. Acad. Sci. USA.* 82:7121–7125.

Sander, A., B.A. Hesser, and V. Witzemann. 2001. MuSK induces in vivo acetylcholine receptor clusters in a ligand-independent manner. *J. Cell Biol.* 155: 1287–1296.

Sanes, J.R., and J.W. Lichtman. 2001. Induction, assembly, maturation and maintenance of a postsynaptic apparatus. *Nat. Rev. Neurosci.* 2:791–805.

Simon, S., E. Krejci, and J. Massoulié. 1998. A four to one association between peptide motifs: four C-terminal domains from cholinesterase assemble with one proline-rich attachment domain (PRAD) in the secretory pathway. *EMBO J.* 17:6178–6187.

Strochlic, L., A. Cartaud, V. Labas, W. Hoch, J. Rossier, and J. Cartaud. 2001. MAGI-1c: a synaptic MAGUK interacting with MuSK at the vertebrate neuromuscular junction. *J. Cell Biol.* 153:1127–1132.

Trinidad, J.C., G.D. Fischbach, and J.B. Cohen. 2000. The Agrin/MuSK signaling pathway is spatially segregated from the neuregulin/ErbB receptor signaling pathway at the neuromuscular junction. *J. Neurosci.* 20:8762–8770.

Watty, A., G. Neubauer, M. Dreger, M. Zimmer, M. Wilm, and S.J. Burden. 2000. The in vivo and in vitro phosphotyrosine map of activated MuSK. *Proc. Natl. Acad. Sci. USA.* 97:4585–4590.